Original Research

Role of xenogenous bovine platelet gel embedded within collagen implant on tendon healing: an *in vitro* and *in vivo* study

Ahmad Oryan[1], Ali Moshiri[2], Abdolhamid Meimandi-Parizi[2] and Nicola Maffulli[3]

[1]Department of Pathology, School of Veterinary Medicine, Shiraz University, Shiraz, 71345, Iran; [2]Division of Surgery and Radiology, Department of Clinical Sciences, School of Veterinary Medicine, Shiraz University, Shiraz, 71345, Iran; [3]University of Salerno, Faculty of Medicine and Surgery, Department of Musculoskeletal Medicine and Surgery, and Centre for Sport and Exercise Medicine, Barts and the London School of Medicine and Dentistry, University of London, Queen Mary, E1 4DG, UK
Corresponding author: Ali Moshiri. Email: dr.ali.moshiri@gmail.com

Abstract

Surgical reconstruction of large Achilles tendon defects is demanding. Platelet concentrates may be useful to favor healing in such conditions. The characteristics of bovine platelet-gel embedded within a collagen-implant were determined *in vitro,* and its healing efficacy was examined in a large Achilles tendon defect in rabbits. Two cm of the left Achilles tendon of 60 rabbits were excised, and the animals were randomly assigned to control (no implant), collagen-implant, or bovine-platelet-gel-collagen-implant groups. The tendon edges were maintained aligned using a Kessler suture. No implant was inserted in the control group. In the two other groups, a collagen-implant or bovine-platelet-gel-collagen-implant was inserted in the defect. The bioelectricity and serum platelet-derived growth factor levels were measured weekly and at 60 days post injury, respectively. After euthanasia at 60 days post injury, the tendons were tested at macroscopic, microscopic, and ultrastructural levels, and their dry matter and biomechanical performances were also assessed. Another 60 rabbits were assigned to receive no implant, a collagen-implant, or a bovine-platelet-gel-collagen-implant, euthanized at 10, 20, 30, and 40 days post injury, and their tendons were evaluated grossly and histologically to determine host-graft interactions. Compared to the control and collagen-implant, treatment with bovine-platelet-gel-collagen-implant improved tissue bioelectricity and serum platelet-derived growth factor levels, and increased cell proliferation, differentiation, and maturation. It also increased number, diameter, and density of the collagen fibrils, alignment and maturation of the collagen fibrils and fibers, biomechanical properties and dry matter content of the injured tendons at 60 days post injury. The bovine-platelet-gel-collagen-implant also increased biodegradability, biocompatibility, and tissue incorporation behavior of the implant compared to the collagen-implant alone. This treatment also decreased tendon adhesion, muscle fibrosis, and atrophy, and improved the physical activity of the animals. The bovine-platelet-gel-collagen-implant was effective in neotenon formation *in vivo,* which may be valuable in the clinical setting.

Keywords: Tendon, tissue engineering, platelet gel, collagen, ultrastructure, biomechanics, host graft interaction

***Experimental Biology and Medicine* 2015; 240: 194–210. DOI: 10.1177/1535370214554532**

Introduction

Surgical reconstruction of a large Achilles tendon defect is challenging.[1,2] Auto- and allografts are current options but have significant limitations.[3,4] In addition, tendon healing has considerable limitations including development of peritendinous adhesions and poor healing response.[5,6]

A tissue-engineered construct could solely be used as a scaffold or it may be combined with healing promoting factors such as growth factors to produce a bioactive graft aiming to optimize its healing capability.[7,8] Platelets are a simple, cost-effective, and practical source of the growth factors.[8,9] The most common form of platelets used in clinical use is platelet rich plasma (PRP).[10] PRP can be produced by one- or two-step centrifugation, resulting in the presence or absence of white blood cells (WBCs) within the solution,[10,11] and directly injected into the lesion. PRP activated by adding coagulating factors, producing an implantable platelet gel[12] (PG), has greater healing efficacy than a PRP solution; in the former, the platelets have longer lifetime in the body than the latter, with more prolonged release of growth factors from the PG.[8,13,14] The growth factors are mainly present in the alpha-granules of the platelets.[14] The alpha-granules are also sources of cytokines, chemokines, and many other proteins variously involved in stimulating

chemotaxis, cell proliferation and maturation, modulating inflammatory molecules, and attracting leukocytes.[15–17]

Recent clinical investigations suggest that platelets may have no effect on tendon healing, while most of the recent animal studies suggest that platelets are effective in such process.[9,12,18–25] This controversy may result from the source of the platelets. The clinical studies used autograft source, while the animal studies have used allograft source of platelets.[8] The effectiveness of platelets may arise from their ability to trigger inflammation, which is important for tendon healing. Allograft platelets might have a greater inflammatory effect than the autografts because of their immunogenic properties. This concept motivated us to test the effectiveness of xenogenous platelets on tendon healing. Bovine platelets are a cost-effective and reliable source of the platelets.

We used a tissue-engineered collagen implant (CI) to reconstruct tendon defects *in vivo*. We enriched this bioimplant with activated xenogenous-based bovine pure platelets to optimize the healing capacity of the implant *in vivo* and to preserve the function of the embedded platelets for a longer period. We hypothesized that bovine platelets may increase the inflammation for a short period; thus, this implant may improve fibroplasia and remodeling phases. In addition, bovine platelets may improve the tenoconductivity, tenoinductivity, tenointegration, and tenogenesis of the collagen implant.

Materials and methods

Ethics

All animals received human care in compliance with the Guide for Care and use of Laboratory Animals published by the National Institutes of Health (NIH publication No. 85-23, revised 1985). The study was approved by the local Ethics Committee of our Veterinary School.

Preparation of the collagen implant

Collagen type I was extracted from the bovine tendon, and its purity was confirmed by SDS/PAGE.[26] The acid solubilized collagen molecules (ASCM-I) were electrospinned onto a dual plate device to produce the large and aligned electrospun collagen fibers. After electrospinning, the ASCM-I were mixed with electrospun collagen fibers and polymerized in an incubator at 4°C for 48 h to produce a three-dimensional (3D) collagen gel. The collagen was aligned under 12 Tesla magnetic fields (CRETA, Grenoble) during polymerization.[27] The collagen composite was cut into several pieces of the same size and shape as the rabbit's Achilles apparatus. The composites were cross-linked after suspension in iso-osmolar 0.1% riboflavin solution, using UV irradiation (wavelength of 365 nm). The final product was repeatedly washed with distilled water, received 100 Gray g-radiation and suspended in ethanol 96% to produce and maintain its sterility until surgery. Given the 3D nature of the scaffold, g-radiation with the above dose was not sufficient to ensure complete sterility of the inner parts of the implant, and higher doses of g-radiation would change the surface activity of the scaffold. Therefore, ethanol 96% was combined with g-radiation to effectively sterilize the inner parts of the scaffold. Ethanol did not have any deleterious effects on surface activity and ultrastructure composition of the scaffold. The morphology of the scaffolds was studied by SEM. Sterility and endotoxin content were tested and confirmed by microbiological and limulus amebocyte lysate tests, respectively.[3]

Preparation of the platelet gel embedding within the collagen implant

Peripheral blood was harvested from healthy bovines and transferred into the sterile EDTA tubes (1.5 mg/mL blood). The animals were free of any infective and zoonotic diseases, and the safety of the blood samples were tested and approved by a certified laboratory (Masoud Lab, Tehran, Iran). On centrifugation of anti-coagulated blood at 1500 rpm ($215 \times g$) for 15 min, the following three layers were formed: RBCs (bottom); WBCs/platelets (buffy coat) (middle); and plasma (top). The plasma and buffy coat layers were suctioned into new tubes and centrifuged again. Three layers including WBCs (bottom), PRP (middle), and PPP (top) were formed. The PPP and PRP were suctioned into new tubes. Three samples were fixed on glass slides and stained with Wright-Giemsa staining; it was confirmed that the samples were free of bovine WBCs and RBCs. The platelets were counted with a standard hemocytometer. After PRP + PPP preparation, the samples were lyophilized and pulverized. The powder was sterilized via UV irradiation and the sterile powder was solved in the sterile PBS (0.9% NaCl). The final platelet concentration per each μL was set to be 2,000,000 platelets (6 to 7 times greater than the physiologic concentration). Two mL of PRP were transferred to a sterile custom-made rectangular dish. The fully dehydrated collagen implants were weighed and then placed in the dish. After 30 min, the scaffolds fully absorbed the solution. Two mL of platelets were activated by bovine thrombin (5000 unit) + 5 mL of $CaCl_2$ 10% with a proportion of 10 platelet solution: 1 activator. This produced a bovine platelet gel embedded within the collagen implant (BPG-CI). The hybrid scaffolds were then air dried and placed in a sterile package for further use. The presence of the platelets and their attachment to the collagen fibers of the implant were confirmed by SEM, TEM, and light microscopy (Figure 1).

In vitro assays

Coagulation profile – activated partial thromboplastin time and prothrombin time. The coagulation profile of the normal blood, PRP produced after first step centrifugation (PRP-F), PRP produced after second step centrifugation (PRP-S), and PRP produced after lyophilization and saline solving procedure (PRP-LS) were measured, using STA Compact MAX instrument (Stago Diagnostica, France) according to the method by Ng *et al*.[28]

Degradation rate. The normal blood clot (NBC), PRP-F, PRP-S, and PRP-LS gel were incubated at 37°C and observed periodically and finally graded after 30 days.

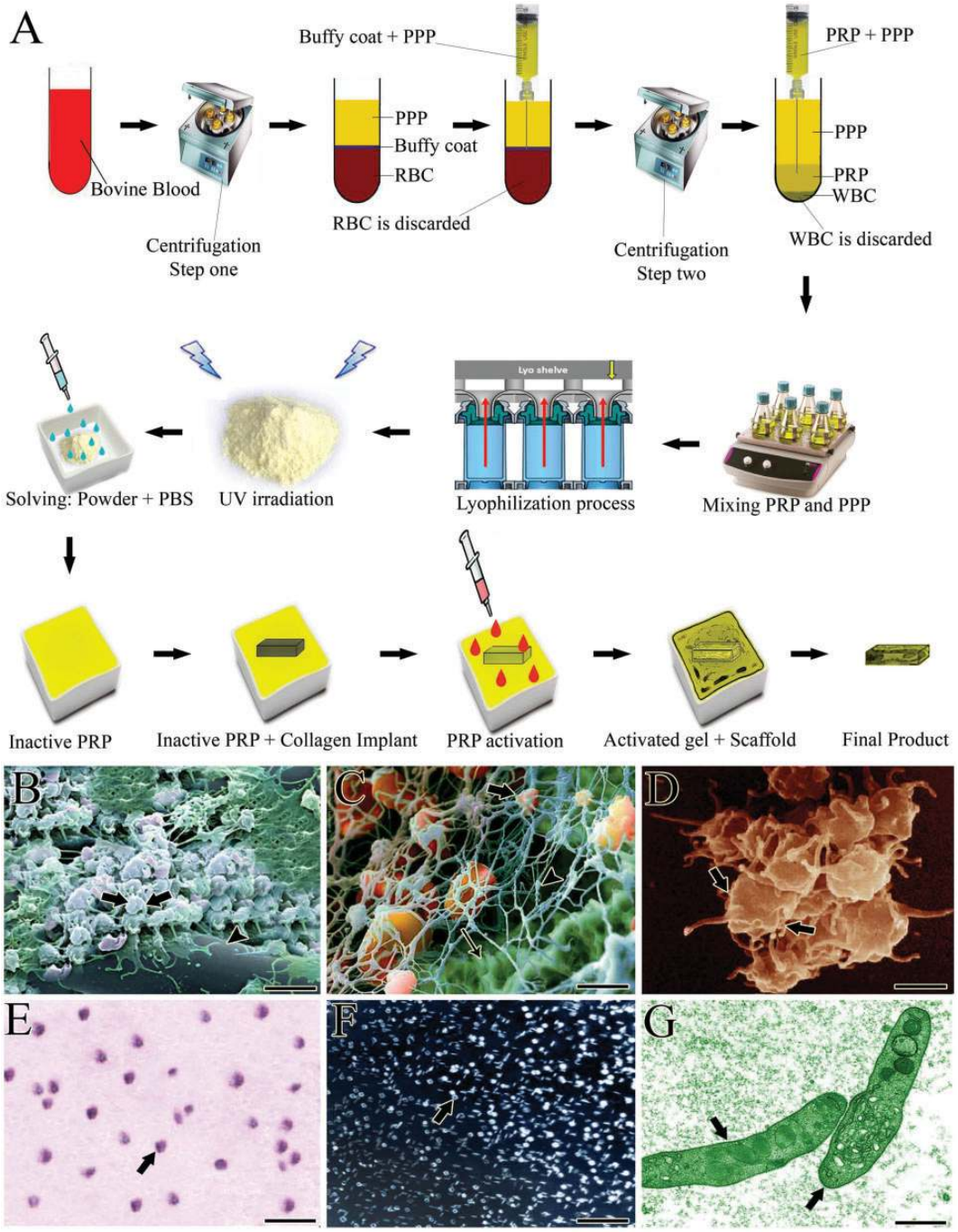

Figure 1 (a) Preparation of the BPG embedded within CI. Each arrow shows a subsequent step. (b) An SEM of the BPG-CI. The platelets (arrows) well attached to the collagen fibers (arrow head). (c) The activated platelets (thick arrow) attached to the fibrin matrix (arrow head) and the collagen fibers (thin arrow). (d) An SEM of the activated and accumulated platelets. (e) Cytologic appearance of the platelets after the second centrifugation. (f) The cytologic section of the bovine PRP by polarized microscopy. (g) The TEM of the bovine platelets after the second centrifugation. Scale bar: (b) 1 μm; (c) 750 nm; (d) 500 nm; (e) 3 μm; (f) 12 μm; (g) 630 nm. (A color version of this figure is available in the online journal.)

Grading was 0 for no changes, 1 for 1–50% degraded, and 2 for 50–100% degraded.

Level of platelet growth factors. The PDGF and IGF-I level of the PRP-F (750,000 platelets/μL, $n=10$), PRP-S (1,500,000 platelets/μL, $n=10$), the PRP-LS (2,000,000 platelets/μL, $n=10$), and the PG (2,000,000 platelets/μL, $n=10$) were measured, using a commercially available Quantikine ELISA kit (DHD00, DG100 respectively, R&D Systems, Minneapolis, MN) according to the manufacturer's protocol as previously described.[14]

Platelet aggregation test. Platelet aggregation was tested by light transmission aggregometry (LTA). In the LTA method (Chrono-log series 400, Harvertown, PA, USA), collagen (3.2 μg/mL) and TRAP-6 (32 μM) (Verum

Diagnostica, München, DE) were used as agonists. The results were expressed as maximal light transmission. The LTA of the PRP-F (750,000 platelets/μL, $n=10$), PRP-S (1,500,000 platelets/μL, $n=10$), and PRP-LS (2,000,000 platelets/μL, $n=10$) were statistically compared.[29]

Live/dead cell assay and immunofluorescence microscopy. Rat skin fibroblasts (cell line CRL-1213) were seeded on the CI and BPG-CI. The scaffolds were grown *in vitro* in a 5% CO_2 incubator at 37°C for 5, 10, and 20 days, with the medium (Dulbecco's Modified Eagle Medium + 10% fetal bovine serum + 20 U/ml penicillin + 20 μg/ml streptomycin) being replaced every 3 days. Cell-scaffold interaction was observed by SEM. Cell viability was determined by live/dead cell assay, using fluorescein diacetate (FDA, Molecular Probes, Invitrogen Corporation) (live) and propidium iodide (Cayman Chemical Company, Michigan, USA) (dead). The scaffolds ($n=10$) with the fluorescence stained cells were viewed under a Nikon fluorescent microscope. The viability index was analyzed as: number of viable cells/total number of cells) × 100.[30]

Cell morphology and cell scaffold interaction were also studied by immunofluorescence microscopy. The scaffolds with cells on a 25-mm coverslip were washed twice with PBS. The cells were fixed in 4% paraformaldehyde, at room temperature (RT), for 60 min. The fixed cells were then washed twice with 0.02% PBS/sodium azide (SA) and permeabilized with 0.2% saponin for 10 min. The non-specific sites were blocked by incubation in 0.02% PBS/1% BSA/0.02% SA for 10 min at RT. The primary antibody (Ab) (anti-Grp78, also known as BiP at a 1:100 dilution) was added to the coverslip to completely cover the surface and allowed to incubate at RT for 45 min. The coverslip was rinsed three times with 0.02% PBS/SA, and then blocked again with PBS/BSA/SA for 10 min. The secondary Ab (Alexa 488 goat anti-rabbit at a 1:100 dilution) was added to the coverslip and incubated at RT for 45 min. The coverslip was rinsed three times with PBS/SA, and then incubated in 2 mL of a DAPI (4′,6-diamidino-2-phenylindole) solution of 0.5 ng mL^{-1} for 15 min. The coverslip was rinsed with PBS/SA, then with deionized water, and mounted on a glass slide with Fluoromount G.[2]

Animals and grouping details

Sixty skeletally mature male White New Zealand rabbits of 12 ± 2 months age and 3.31 ± 0.22 kg body weight were randomly selected as the experimental groups to investigate the effectiveness of BPG on the remodeling phase of tendon healing at 60 days post injury (DPI). In each animal, the left hind leg was selected to produce a large tendon defect and the right leg was left intact. The animals were randomly assigned to three groups: control (defect without implant) ($n=20$), treated with collagen implant (TCI) ($n=20$), and treated with collagen-platelet gel implant (TC-PGI) ($n=20$). Another 60 animals were used as a pilot model to determine the host-graft interaction mechanism and the quality of tendon healing at earlier stages of tendon healing. The pilot animals were randomly divided into three groups: control ($n=20$), TCI ($n=20$), TC-PGI ($n=20$). Each group was then divided into four subgroups of 10 ($n=5$), 20 ($n=5$), 30 ($n=5$), and 40 ($n=5$) DPI.

Premedication and anesthesia

Premedication was provided by intra-muscular injection of 1 mg/kg acepromazine maleate. The animals were anesthetized by intra-muscular injection of 15 mg/kg Ketamine + 0.05 mg/kg Xylazine hydrochloride (all from Alfasan Co, Woerden, Netherlands). Given the analgesic effects of Xylazine, no further intra-operative analgesia was provided.[27]

Injury induction and surgical reconstruction

The left hind limb of the animals was prepared aseptically. After a longitudinal skin incision over the Achilles tendon complex, 2 cm of the Achilles tendon (all the three strands) with the covering paratenon were completely excised by transverse incisions, approximately 5 mm distal to the gastrocnemius-soleus muscle and 5 mm proximal to the calcaneal tuberosity. Primary reconstruction of the tendon was undertaken, using double-strand modified Kessler core pattern (PDS 0-4, Ethicon, INC.1997, Johnson & Johnson, USA). This aligned the remaining tendon extremities in a normal anatomical position, and produced a 2-cm gap between the tendon ends. For insertion of the implants in the tendon gap, a double-strand suture was passed through the longitudinal axis of the implants. The subcutaneous tissue and skin over the lesion were closed in a routine fashion (Figure 2). Postoperative analgesia with fentanyl (Matrifen, Roskilde, DK; 0.0015 mg/kg/h) was provided for 3 days via a transdermal patch applied to the depilated and sutured skin.

Clinical examinations

Tarsal flexion degree, weight distribution pattern, heel and toe position, pain, and swelling were scored weekly (Table S1). The animals were monitored weekly for their behavior and physical status.

Bioelectrical characteristics

Direct transmission electrical current (DTEC; micro-amp) and tissue resistance to direct transmission electrical current (TRDTEC; micro-ohm) of the injured control tendons (ICTs; no implant), injured treated tendons with collagen implant (ITTCs), injured treated tendons with collagen implant-platelet gel (ITTC-PGs) and their normal contralateral tendons (NCTs) were weekly measured with a digital multi pen type meter (Mastech, Seoul, South Korea).[31]

PDGF Level

Immediately before euthanasia, 10 mL of blood were collected from each animal, placed in test tubes without EDTA, and centrifuged for 10 min at 3500 rpm to separate the serum. Serum PDGF concentration was measured with a commercial ELISA kit: Platelet-Derived Growth Factor AA (PDGF-AA) and AB Immunoassay (Biotrend

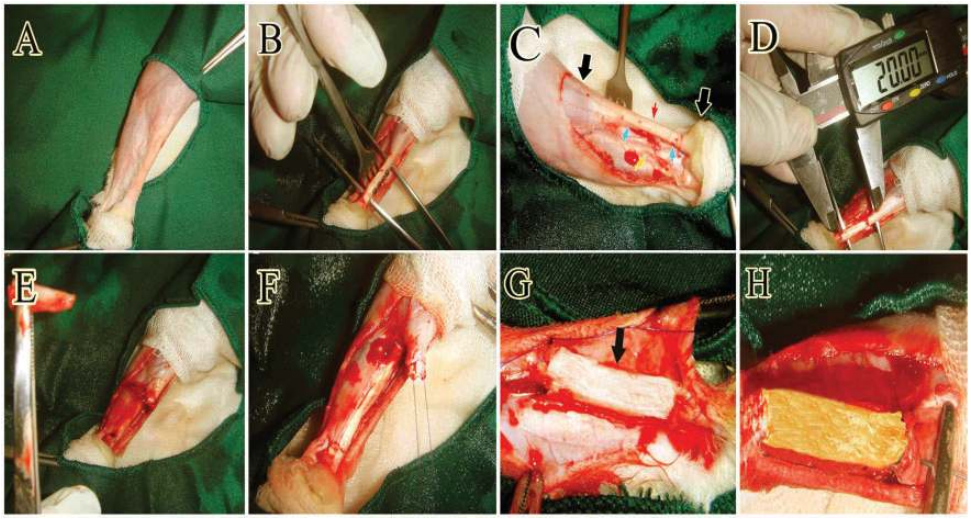

Figure 2 Surgical operation. (a) Surgical site and preparation method. (b) Skin incision and exposure of the Achilles tendon apparatus (ATA). (c) The black arrows point to the gastroc. soleus muscle proximally and calcaneal tuberosity distally. The red arrow points to the ATA. The blue arrows point to the segment to be removed, and the yellow arrow points to the *tibialis posterior* tendon. (d and e) Two cm of the ATA was measured and removed by sharp dissection. (f) A modified Kessler suture was anchored at the edges of the remaining tendon. (g and h) The CI and BPG-CI were inserted. (A color version of this figure is available in the online journal.)

Chemicals, LLC136 South Holiday Road, Unit C, Destin, FL 32550).[32]

Euthanasia

The animals were anesthetized by intra-muscular injection of 15 mg/kg Ketamine + 2 mg/kg Xylazine + 1 mg/kg Acepromazine maleate (All from, Alfasan Co, Woerden, Netherlands). Then, they were euthanized by intra-cardiac injection of 1 mg/kg Gallamine triethiodide (Specia Co., Paris, France).

Sample collection

Each injured tendon and its normal contralateral tendon (NCT) was dissected and assessed for gross pathology ($n = 20^{L}$ and 20^{R} for each experimental group, $n = 5^{L}$ and 5^{R} for the pilot groups at each time interval). The samples from each group were randomly divided into two equal subgroups. Subgroup 1 ($n = 10^{L}$, 10^{R}) was used for biomechanical testing and subgroup 2 ($n = 10^{L}$, 10^{R}) was used for morphological and dry matter content analyses. The tendons in subgroup 2 were longitudinally divided into two parts. Part A (medial part) was used for histopathology and part B (lateral part) for TEM, and determination of the dry matter content.

Gross pathology

Hyperemia, peritendinous adhesion, general appearance, muscle atrophy, and fibrosis and tendon diameter were scored and measured (Table S2).[3]

Histopathologic and histomorphometric analysis

After fixation in 10% neutral buffered formalin, the samples were washed, dehydrated, cleared, embedded in paraffin wax, sectioned at 4 μm in thickness, and stained by H&E.[4] The samples were examined by a light microscope (Olympus, Tokyo, Japan). The photomicrographs were captured from the histologic fields and transferred to the computer software (Adobe Photoshop CS-5, Ca, USA) for digital analysis ($n^{\text{sample}} = 10$, $n^{\text{histopathologic section}} = 5$, $n^{\text{histopathologic field}} = 5$, totally 250^{L} and 250^{R} histopathologic fields for each group). Total cellularity, immature tenoblasts, mature tenoblasts, tenocytes, neutrophils, lymphocytes, macrophages, plasma cells, and blood vessels of the tendon proper (mid portion) were counted (magnification 200×).[27]

The collagen mass density (%) was analyzed by computer software (Image J, NIH, CA, USA). The crimp pattern, tissue alignment and perivascular edema were scored (Table S3).

Transmission and scanning electron microscopy

The mid portion of the tendon proper was used for SEM and TEM examinations. For SEM, the samples were fixed in cold 4% glutaraldehyde, dehydrated with hexamethyldisilazane, and finally gold coated.[3] For TEM, the samples were fixed in cold 4% glutaraldehyde, dehydrated in a graded series of increasing concentration of ethanol, and embedded in epoxy resin 811 (TAAB, CO., London, UK). Transverse sections with 70–80 nm thickness were prepared, and standard methods were employed for production of the ultramicrographs (number of tendon samples in each group = 10 left, 10 right, number of ultrathin sections in each tendon = 5, number of ultramicrographs in each ultrathin section = 5; in total, 250 L and 250 R ultramicrographs in each group).[30] The number of collagen fibrils and elastic fibers were counted in all the ultramicrographs (magnification 39,000×). The transverse diameter of all the collagen fibrils of all the ultramicrographs and the transverse diameter of one hundred elastic fibers were measured.

The collagen fibrils' density was measured as: transverse area of the fibrils/total area (nm^2) × 100. Morphometric measurements were performed, using standard morphometric software (Image J, NIH, CA, USA and Adobe Co. Photoshop CS 5 extended. NY, USA). The mesenchymal cells were divided into tenoblasts and tenocytes, based on their morphology. In each group, 100 cells were counted, and the number of tenocytes was reported as percentage of total mesenchymal cells. Alignment and maturity of the collagen fibrils and elastic fibers were scored (Table S4).

Dry matter content

Dry matter content was calculated as: dry weight/wet weight × 100.[3]

Biomechanical testing

The distal end of the Achilles tendons together with a portion of the calcaneus were detached distally, and 3 cm of gastroc. soleus muscle belly with its Achilles insertion were excised proximally. The tendons were collected in moist sterile gauze swabs soaked in 0.9% normal saline, wrapped in foil, and placed in a plastic bag to stop further water evaporation immediately after the animal was euthanized, and then quickly stored at −70°C for 3 days, before biomechanical tests were performed. The specimens were thawed at RT prior to biomechanical testing. Care was taken to keep the tendon moist with saline-soaked gauze at all times prior to and during testing. The tendons were mounted vertically on a materials testing system (Instron® Tensile Testing Machine, London, UK). We used a dual-cryogenic fixation assembly, which held the tendon securely at both ends. Each tendon was loaded by elongating it at a displacement rate of 10 mm s^{-1} until a 50% decrease in load was detected. Load and crosshead displacement data were recorded at 1500 Hz, and load-deformation and stress–strain curves were generated for each specimen, using Test Works 4 software (SUME Systems Corporation).[31]

Statistical analysis

All quantitative values were expressed as mean ± SD and the measured values in each group were statistically tested, using paired-sample *t*-test. The measured values between multiple groups were tested, using one-way ANOVA with its subsequent Tukey's *post hoc* tests. All scored values were expressed as median (minimum–maximum). Kruskal-Wallis *H* test was performed to analyze the scored values. $P < 0.05$ was considered statistically significant.

Results

In vitro results

Coagulation profile. Regarding the APTT, no significant differences were seen between the NBC and PRP-F and also between PRP-F and PRP-S ($P > 0.05$). However, lyophilizaion and the saline solving procedure (LSp) significantly increased prothrombin and clotting time of the PRP-LS compared to the controls ($P < 0.05$) (Figure 3).

Degradation rate. After the second step centrifugation, the degradation rate (DR) of the PRP significantly decreased compared to the controls ($P = 0.001$). LSp significantly decreased the DR of the BPG compared to the controls ($P = 0.001$) (Figure 3).

Light transmission aggregometry. There were no significant differences between the LTA of PRP-F and PRP-S ($P > 0.05$). There were also no significant differences between the LTA of the PRP-S and those PRP-LS ($P > 0.05$) (Figure 3).

Level of the platelet growth factors. After the second step centrifugation, the PDGF AB and IGF-I level of the PRP-S were significantly higher than the PRP-F ($P = 0.001$). After LSp, the PDGF AA and IGF-I level of the PRP-LS significantly reduced compared to PRP-S ($P = 0.001$). Activation of the PRP-LS to BPG significantly increased the PDGF AA and IGF-I level of the samples compared to the controls ($P = 0.001$) (Figure 3).

Cell viability. Embedding the BPG within the CI significantly increased the number of the viable cells in the CI-BPG compared to the CI ($P = 0.001$) at 5 to 20 days after cell seeding and culture. Platelets improved cellular proliferation, their maturation, and matrix production (Figures 3 and 4).

In vivo results

Clinical findings. The treated animals gained superior scored values for tarsal flexion degree, weight distribution, heel and toe position, and physical activity compared to the control animals ($P < 0.05$). Those animals treated with CI-BPG exhibited greater tarsal flexion and weight distribution than those treated with CI alone ($P < 0.05$).

Bioelectrical characteristics. At 7 DPI, the DTEC of all the lesions significantly increased compared to those at 0 DPI. At this stage, the ICTs showed significantly higher DTEC than the ITTCs and ITTC-PGs ($P = 0.001$). At 14 DPI, the DTEC of the ICTs started to reduce while the DTEC of the ITTCs and ITTC-PGs significantly increased compared to the measured values recorded at 7 DPI ($P = 0.013$, $P = 0.002$, respectively). At 14 DPI, although the DTEC of the ITTCs increased and the DTEC of the ICTs decreased when compared to 7 DPI, the DTEC of the ITTCs was still significantly lower than the ICTs. At 20 DPI, the DTEC of the ITTCs and ITTC-PGs was significantly lower than those of the 14 DPI, and also than the ICTs at 20 DPI ($P = 0.001$ for all). At 30 and 60 DPI, the DTEC of all the lesions gradually reduced compared to 20 DPI. At these stages, the DTEC of the ITTCs and ITTC-PGs was significantly lower than the ICTs, the DTEC of the ITTC-PGs was significantly lower than the ITTCs and was closer to normal values ($P = 0.001$ for all) (Figure 5).

At 7 DPI, the TRDTEC of all the lesions significantly decreased compared to normal value ($P = 0.001$ for all). At 7 and 14 DPI the TRDTEC of the ICTs was significantly lower than the ITTCs and ITTC-PGs ($P = 0.001$ for both).

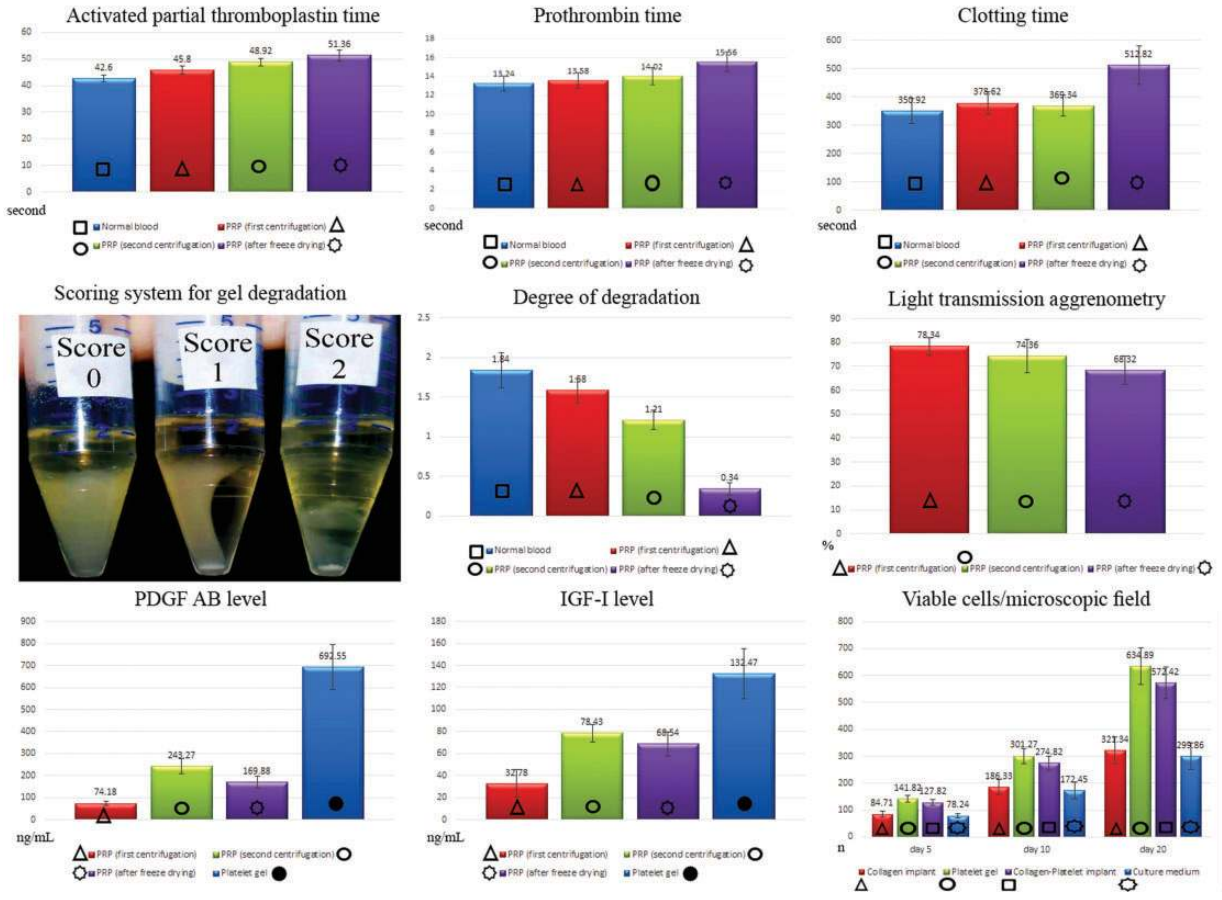

Figure 3 *In vitro* characteristics of the bovine platelets. (A color version of this figure is available in the online journal.)

At 20 DPI, the TRDTEC of the lesions significantly increased compared to those at 14 DPI ($P = 0.001$ for all); the TRDTEC of the treated lesions was significantly higher than the ICTs ($P = 0.001$ for both). At 30 DPI, the TRDTEC of all the lesions increased compared to those at 20 DPI, but this difference was only significant for the ITTC-PGs ($P < 0.05$). At this stage, the TRDTEC of the ITTCs was significantly higher than the ICTs ($P = 0.001$) and the TRDTEC of the ICTs and ITTCs was significantly lower than the ITTC-PGs ($P = 0.001$ for both). The same pattern was seen at 60 DPI so that the ITTC-PGs had the highest TRDTEC when compared to the ITTCs and ICTs ($P = 0.001$) (Figure 5).

Serum PDGF level. At 60 DPI, the serum PDGF of all the animals was higher than normal value ($P = 0.001$ for all). At this stage, the CI-treated animals had significantly higher serum PDGF AA and AB level compared to the control animals ($P = 0.001$). At 60 DPI, the serum PDGF level of the BPG-CI treated animals was significantly higher than those that were treated with CI or left untreated ($P = 0.001$ for both) (Figure 5).

Gross pathology. No considerable healing response occurred in the ICTs so that the healing tissue was edematous and hyperemic and the defect area was not filled with the fibrous connective tissue. At 60 DPI only a loose areolar connective tissue which tightly adhered to the surrounding fascia covered the defect area and the healing tendon was elongated. In the ICTs, the tendon edges were necrotized at the inflammatory stage and the gastroc. soleus muscle atrophied and a severe muscle fibrosis developed. In contrast, in the treated lesions, a severe inflammatory reaction occurred around the implants shortly after implantation. Compared to the ITTCs, the ITTC-PGs showed more inflammatory reaction in the inflammatory phase. The ability of the implants to trigger the inflammation produced a strong fibroplastic response in the defect area so that the implants were covered by the new granulation tissue soon after tendon injury (e.g. after 10 days). Although the inflammation was higher in the ITTC-PGs than the ITTCs, in the ITTC-PGs, the implant was absorbed and replaced by a new tendon faster than the ITTCs. The ITTC-PGs had a more homogenous fibroplastic surface especially at 60 DPI than the ITTCs. Less muscle atrophy and fibrosis together with less peritendinous adhesions were observed in the treated lesions compared to the controls. At 60 DPI, the ICTs had smaller transverse diameter (short transverse diameter [S]: 1.19 ± 0.29 mm, large transverse diameter [L]: 2.24 ± 0.49 mm) than the ITTCs (S: 2.12 ± 0.25 mm; L: 3.31 ± 0.36 mm) and ITTC-PGs (S: 3.14 ± 0.33 mm; L: 3.91 ± 0.42 mm) ($P = 0.001$ for all). At this stage, the short

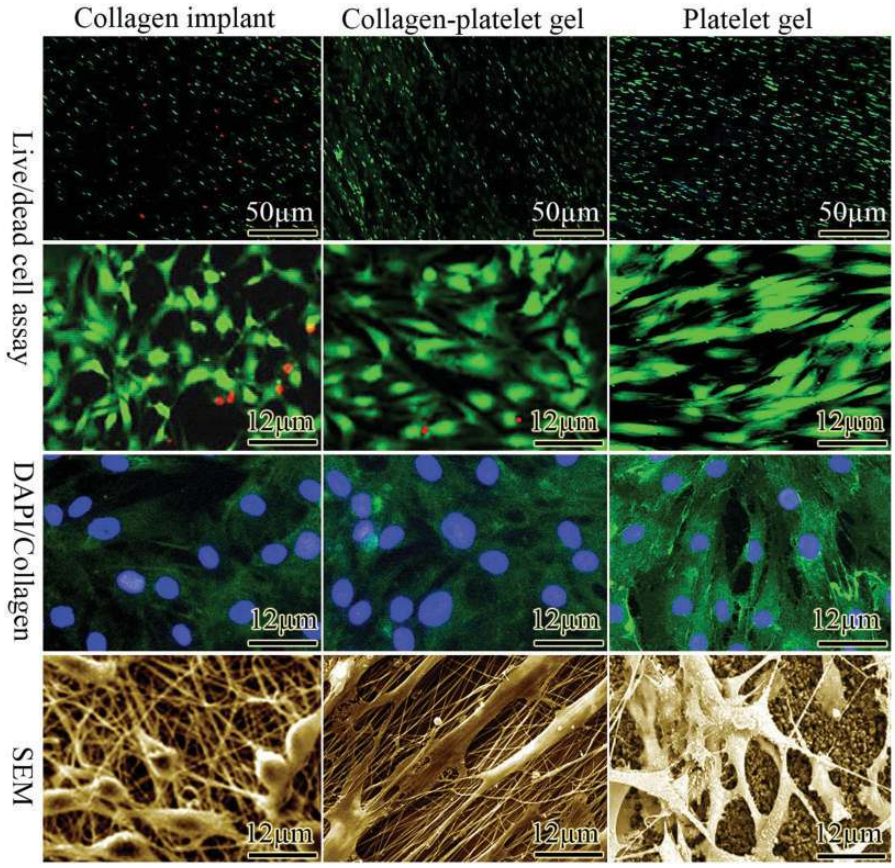

Figure 4 Live/dead cell assay, immunoflorescent microscopy, and SEM of the cultured fibroblasts on CI, BPG-CI, and BPG. The BPG increased cellular migration, proliferation, and matrix production *in vitro*. (A color version of this figure is available in the online journal.)

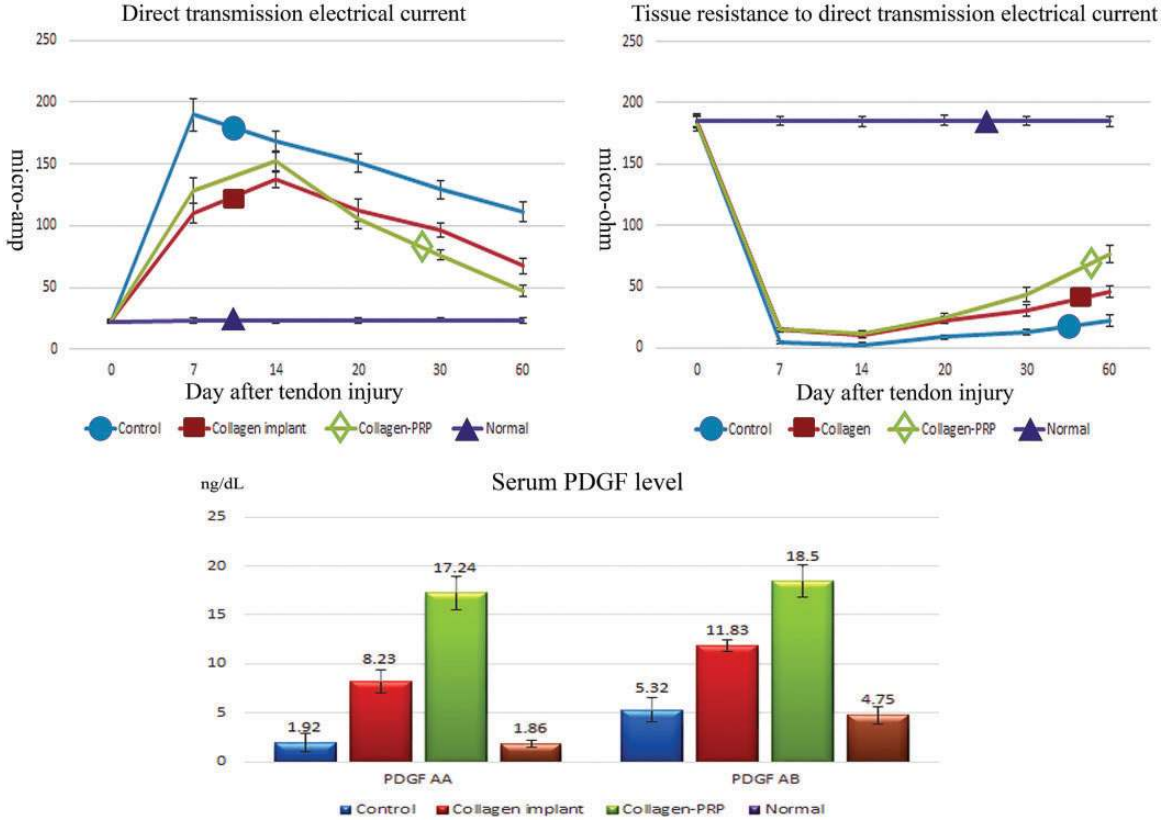

Figure 5 The BPG significantly reduced DTEC and increased TRDTEC of the ITTC-PGs and approximated them to the normal values in comparison to the controls. At 60 DPI, those animals treated with BPG-CI showed significantly higher serum PDGF level than controls. (A color version of this figure is available in the online journal.)

transverse diameter of the ITTC-PGs was significantly higher than the ITTCs ($P = 0.001$). In addition, the transverse diameters of the ITTC-PGs were comparable to the NCTs (S: 3.38 ± 0.27 mm; L: 3.96 ± 0.49 mm; $P > 0.05$). The ITTCs-PGs and ITTCs showed significantly superior scored values for peritendinous adhesion $(1(0–2)^{\text{ITTC-PGs}}$ vs. $2.5(1–2)^{\text{ITTCs}}$ vs. $3(2–3)^{\text{ICTs}}$; $P = 0.044$, $P = 0.009$, respectively), hyperemia $(1(0–1)^{\text{ITTC-PGs}}$ vs. $1.5(2–3)^{\text{ITTCs}}$ vs. $3(2–3)^{\text{ICTs}}$; $P = 0.029$, $P = 0.001$, respectively), muscle fibrosis $(3(1–3)^{\text{ITTCs}}$ vs. $1(0–2)^{\text{ITTC-PGs}}$ vs. $3(3–4)^{\text{ICTs}}$, $P = 0.042$, $P = 0.001$, respectively), muscle atrophy $(1.5(1–2)^{\text{ITTC-PGs}}$ vs. $3(0–3)^{\text{ITTCs}}$ vs. $3(2–4)^{\text{ICTs}}$, $P = 0.049$, $P = 0.007$, respectively), and general appearance of the injured tendons $(2(0–2)^{\text{ITTC-PGs}}$ vs. $2(0–3)^{\text{ITTCs}}$ vs. $3(1–4)^{\text{ICTs}}$, $P = 0.044$, $P = 0.019$, respectively) compared to the ICTs (Figure 6).

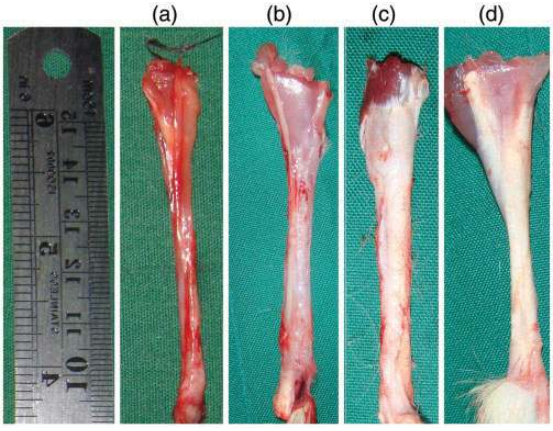

Figure 6 (a) ICTs (no implant). (b) ITTCs. (c) ITTC-PGs. (d) NCTs. At 60 DPI, the PG considerably decreased tendon hyperemia, peritendinous adhesions, muscle fibrosis, and atrophy and it increased the homogeneity and density of the newly formed fibrous connective tissue in the defect area when compared to the controls. (A color version of this figure is available in the online journal.)

Histologic and histomorphometric analyses. In the ITTCs, the inflammatory cells accumulated in the peripheral parts of the CI were degrading the scaffold, at 10 DPI. The new granulation tissue covered the CI at this stage. In contrast, in the ITTC-PGs, the inflammatory cells were evenly distributed throughout the BPG-CI at 10 DPI. At 20 DPI, some parts of the CI were highly invaded by inflammatory cells but some collagen remnants (CRs) were present with no inflammatory reaction. In contrast to the ITTCs, the CRs in the ITTC-PGs were free of inflammatory cell reaction and the new connective tissue filled the free spaces between them. These free spaces were those areas that were previously degraded by the inflammatory cells or were lysed by the inflammatory mediators. At 30 DPI in the ITTCs, some parts of the CI were infiltrated by the tenoblasts and accepted as parts of the neotenon, but the newly regenerated tissue which surrounded the CRs were immature and consisted of immature vessels and low collagen density. In contrast, in the ITTC-PGs, the CRs, were well infiltrated by the host tenoblasts and the newly regenerated tissue which covered the CRs was a mature connective tissue consisting of aligned collagen fibers and a combination of mature tenoblasts and tenocytes. At 40 DPI in the ITTCs, some other CRs were also degraded and replaced by the new connective tissue so that there were two distinct areas of the mature and immature collagen fibers. In contrast to the ITTCs, in the ITTC-PGs, most of the neotenon was filled with the mature collagen fibers. At 60 DPI, the treated lesions were tendinous in nature, with aligned collagen fibers which were oriented between the gastroc. soleus and calcaneal tuberosity. In contrast, in the ICTs only a loose areolar connective tissue formed and several inflammatory and immature mesenchymal cells were present in the highly vascular but haphazardly organized newly formed granulation tissue (Figure 7). At 60 DPI, the continuity of the PDS suture was completely lost, the suture

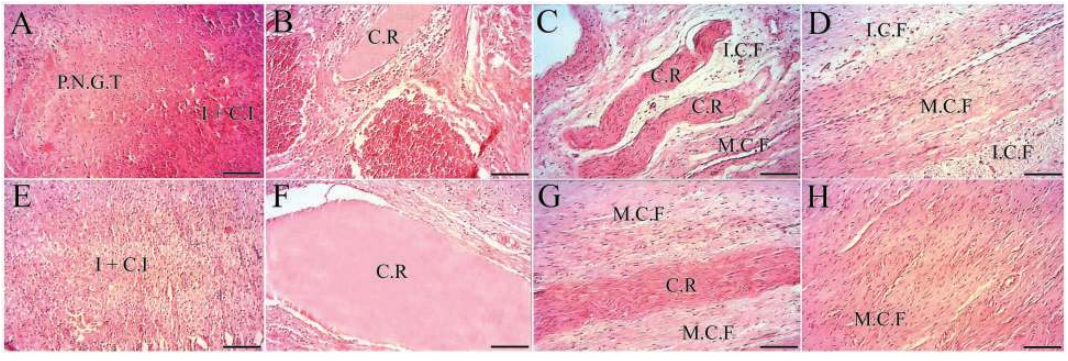

Figure 7 Histopathological evaluation of host-graft interaction at various stages of tendon healing. (a to d) ITTCs at 10, 20, 30, and 40 DPI. (e to h) ITTC-PGs at 10, 20, 30, and 40 DPI, respectively. At 10 DPI, in the ITTCs (a), the inflammatory cells (I) were accumulated in the peripheral parts of the collagen implant (CI) and were degrading it. The peripheral new granulation tissue (PNGT) has covered the CI at this stage. In contrast (a), in the ITTC-PGs (e), the inflammatory cells were evenly distributed throughout the implant (I + CI) at 10 DPI. At 20 DPI, some parts of the CI were invaded by high accumulation of inflammatory cells (b) but some collagen remnants (CR) remained with no inflammatory reaction. In contrast to the ITTCs, in the ITTC-PGs, the CR were free of inflammatory cells accumulation (f). The newly developed connective tissue filled the free spaces between the CR. At 30 DPI, in the ITTCs, some parts of the CR were infiltrated by the tenoblasts and were accepted as parts of the neotenon, but the newly regenerated tissue which surrounded the CR were immature in nature, consisting of immature vessels and low collagen density (**C**). In contrast to the ITTCs, in the ITTC-PGs, the CR were well infiltrated by the host tenoblasts and the newly regenerated tissue which covered the CR was a mature connective tissue (MCT) consisting of aligned collagen fibers and a combination of tenoblast and tenocytes (g). At 40 DPI, in the ITTCs, some other CR were also degraded and replaced by the new connective tissue so that there were two distinct areas of the mature (MCF) and immature (ICF) collagen fibers (d). In contrast to the ITTCs, most of the new tendon, in the ITTC-PGs, was filled with the mature collagen fibers (MCF) at this stage (h). (A color version of this figure is available in the online journal.)

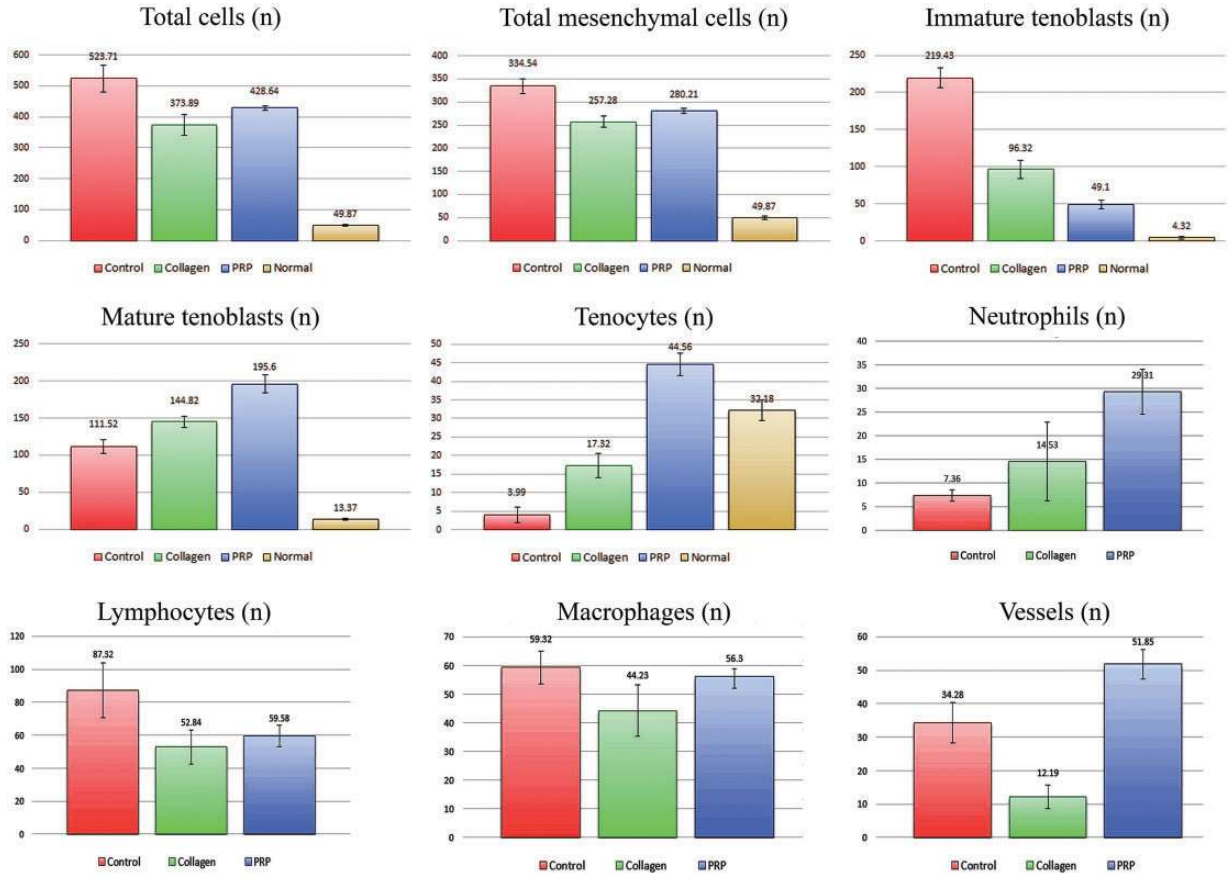

Figure 8 Differential cell counts in the histology sections of the injured healing tendons at 60 DPI. In each group: *n* tendon samples = 10; *n* histologic sections = 5; *n* histologic field = 5; totally 250 field. The results were expressed as mean ± standard deviation. (A color version of this figure is available in the online journal.)

was partially degraded but few remnants were seen at the myotendinous junction.

At 60 DPI, the ICTs showed the highest cellularity, total mesenchymal cells, immature tenoblasts, and lymphocytes compared to the ITTCs and ITTC-PGs ($P = 0.001$ for all). In contrast to the ICTs, the ITTCs and ITTC-PGs had significantly more mature tenoblasts and tenocytes ($P = 0.001$ for both). In addition, the ITTC-PGs had significantly less immature tenoblast but significantly higher cellularity, mature tenoblast, tenocyte, neutrophil, and mature blood vessels when compared to the ITTCs ($P = 0.001$ for all). Moreover, the ITTC-PGs had higher macrophage count than the ITTCs, but the differences were not statistically significant ($P > 0.05$) (Figure 8).

The ITTC-PGs and ITTCs showed significantly superior scored values for collagen fiber alignment $(0(0–1)^{\text{ITTC-PGs}}$ vs. $1(1–3)^{\text{ITTCs}}$ vs. $3(2–3)^{\text{ICTs}}$, $P = 0.001$ for both), perivascular edema $(0(0–1)^{\text{ITTC-PGs}}$ vs. $0.5(0–1)^{\text{ITTCs}}$ vs. $2(2–3)^{\text{ICTs}}$, $P = 0.001$, $P = 0.012$, respectively), tissue maturity $(0.5(0–1)^{\text{ITTC-PGs}}$ vs. $1.5(1–2)^{\text{ITTCs}}$ vs. $3.5(2–4)^{\text{ICTs}}$, $P = 0.001$, $P = 0.044$, respectively), crimp pattern $(1(0–2)^{\text{ITTC-PGs}}$ vs. $1.5(1–2)^{\text{ITTCs}}$ vs. $4(4–4)^{\text{ICTs}}$, $P = 0.001$ for both), and vascularity $(0.5(0–2)^{\text{ITTC-PGs}}$ vs. $1.5(1–3)^{\text{ITTCs}}$ vs. $4.5(4–5)^{\text{ICTs}}$, $P = 0.001$ for both) compared to the ICTs. Less muscle fibrosis and atrophy were observed in the treated lesions compared to the ICTs at 60 DPI (Figure 9).

Transmission electron microscopy. At 60 DPI, the ITTCs had significantly higher number and transverse diameter of the collagen fibrils in the ranges of 0 to 64 and 65 to 102 nm, total number and transverse diameter of the collagen fibrils, collagen fibrils' density, and number of elastic fibers than the ICTs ($P = 0.001$ for all). Compared to the ICTs and ITTCs, the ITTC-PGs had significantly higher number and greater transverse diameter of collagen fibrils in the ranges of 0 to 64, 65 to 102, 103 to 153, 154 to 256 nm, number and transverse diameter of total collagen fibrils, collagen fibrils' density, and number of elastic fibers than the ITTCs and ICTs ($P = 0.001$ for all) (Table 1, Figure 10).

Compared to the ICTs, the ITTCs and ITTC-PGs showed significantly superior scored values for alignment $(3.5(3–4)^{\text{ICTs}}$ vs. $2.5(1–3)^{\text{ITTCs}}$ vs. $1(0–2)^{\text{ITTC-PGs}}$; $P = 0.049$, $P = 0.001$, respectively), collagen maturity $(4(4–4)^{\text{ICTs}}$ vs. $3(3–3)^{\text{ITTCs}}$ vs. $2(1–2)^{\text{ITTC-PGs}}$; $P = 0.042$, $P = 0.009$, respectively), and elastic fiber maturity $3(3–3)^{\text{ICTs}}$ vs. $2(1–2)^{\text{ITTCs}}$ vs. $0.5(0–1)^{\text{ITTC-PGs}}$; $P = 0.035$, $P = 0.001$, respectively).

Biomechanical findings. The ITTCs had significantly higher maximum tensile load, yield load, stiffness, and elastic modulus and lower maximum strain compared to the ICTs ($P = 0.001$ for all), at 60 DPI. At this stage, the ITTC-PGs had significantly higher maximum tensile load, yield load, stiffness, maximum tensile strength, and elastic

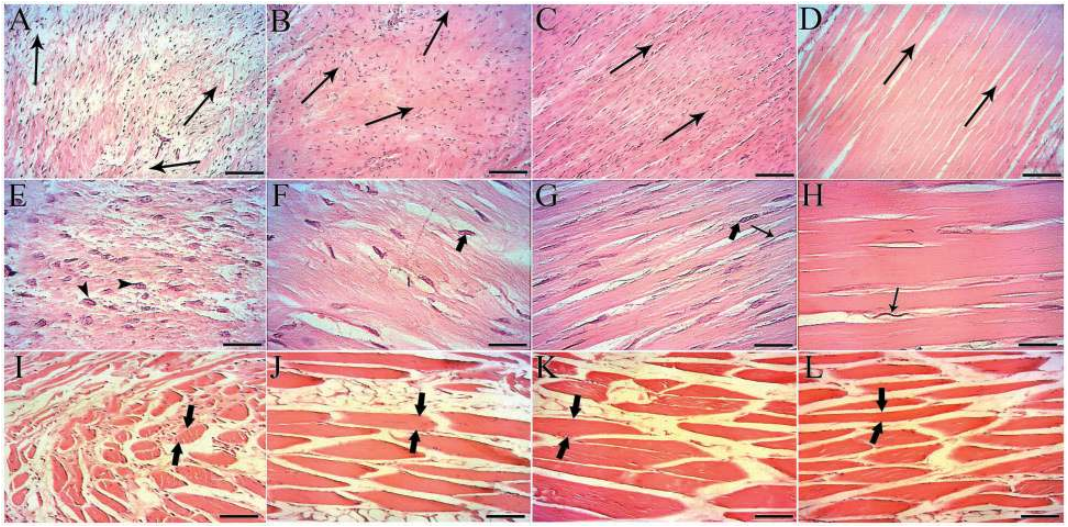

Figure 9 Histopathologic characteristics of the injured and normal tendons at 60 DPI. (a), (e), (i): ICTs; (b), (f), (j) ITTCs; (c), (g), (k): ITTC-PGs; (d), (h), (l): NCTs. (a to d) Longitudinal sections of the tendons, low magnification view (Scale bar = 50 μm); (e to h) longitudinal sections of the tendons, high magnification view (Scale bar = 12.5 μm); (i to l) the histologic sections of the gastroc. soleus muscle (Scale bar = 50 μm). (a to d) The long thin arrows show the orientation of the collagen fibers. At 60 DPI, only a loose areolar connective tissue, consisting of immature tenoblasts and low-density collagen material, had formed in the ICTs (a and e). At this stage, a tendon-like tissue was formed in the ITTCs and the collagen fibers were well developed and the cells were a combination of immature (arrows head) and mature tenoblasts. However, the collagen fibers were not completely aligned because they laid at various directions (b and f). In contrast to the ITTCs, the newly developed tendon-like tissue in the ITTC-PGs was more mature, consisting of highly aligned collagen fibers and a combination of mature tenoblasts (thick arrows) and tenocytes (thin arrows) laid along the direction of the collagen fibers (c and g). In NCTs, large collagen fibers were oriented unidirectionally (arrows) and few tenocytes organized along these aligned collagen fibers (d and h). The ICTs showed severe muscle atrophy and fibrosis so that the muscle fibers (arrow) were small and were severely infiltrated by fibrous connective tissue (i). The CI reduced muscle fibrosis and atrophy (j). The BPG-CI considerably increased the muscle fiber size (k) when compared to the NCTs (l). Color staining: H&E. (A color version of this figure is available in the online journal.)

Table 1 Ultrastructural characteristics of the injured healing tendons after 60 days of tendon injury

	Control (defect) (1)	Collagen implant (2)	Platelet gel embedded in the collagen implant (3)	*P* value (1) vs. (2)	*P* value (1) vs. (3)	*P* value (2) vs. (3)
Number of fibrils (in the range of 0–64 nm)	350.26 ± 21.71	549.8 ± 26	723.59 ± 32.00	0.001	0.001	0.001
Number of fibrils (in the range of 65–102 nm)	0	48.95 ± 8	112.49 ± 12.23	0.001	0.001	0.001
Number of fibrils (in the range of 103–153 nm)	0	0	43.57 ± 5.61	0.001	0.001	0.001
Number of fibrils (in the range of 154–256 nm)	0	0	8.68 ± 2.5	0.001	0.001	0.001
Total number of fibrils (in the range of 0–256 nm)	350.26 ± 21.71	590.08 ± 28.81	914.44 ± 47.08	0.001	0.001	0.001
Transverse diameter of fibrils (in the range of 0–64 nm)	28.72 ± 2.46	45.28 ± 5.19	58.39 ± 3.08	0.001	0.001	0.001
Transverse diameter of fibrils (in the range of 65–102 nm)	0	72.96 ± 4.68	94.42 ± 4.58	0.001	0.001	0.001
Transverse diameter of fibrils (in the range of 103–153 nm)	0	0	118.18 ± 4.17	0.001	0.001	0.001
Transverse diameter of fibrils (in the range of 154–256 nm)	0	0	166.78 ± 6.94	0.001	0.001	0.001
Total transverse diameter of fibrils (in the range of 0–256 nm)	28.72 ± 2.46	47.96 ± 1.6	66.95 ± 2.31	0.001	0.001	0.001
Fibril Density (fibrils area/area of ultramicrographs) (%)	47.15 ± 4.17	66.23 ± 5.28	81.62 ± 4.64	0.001	0.001	0.001
Number of elastic fibers	2.33 ± 0.66	8.93 ± 1.46	16.39 ± 1.29	0.001	0.001	0.001

(continued)

Table 1 Continued

	Control (defect) (1)	Collagen implant (2)	Platelet gel embedded in the collagen implant (3)	*P* value (1) vs. (2)	*P* value (1) vs. (3)	*P* value (2) vs. (3)
Transverse diameter of immature tenoblasts (nm)	8429.48 ± 557.24	6764.45 ± 345.7	5834.2 ± 698.12	0.001	0.001	0.204
Transverse diameter of mature tenoblasts (nm)	3787.39 ± 146.91	3582.81 ± 148.18	2904.54 ± 122.21	0.592	0.001	0.001
Transverse diameter of tenocytes (nm)	1848.42 ± 74.01	1673.26 ± 98.62	1296.44 ± 64.78	0.158	0.001	0.001
Transverse diameter of elastic fibers (nm)	56.26 ± 7.58	113.03 ± 16.94	190.03 ± 9.68	0.001	0.001	0.001

One-way ANOVA with a *post hoc* Tukey's test was used to analyze the differences between the groups. $P < 0.05$ was considered statistically significant.

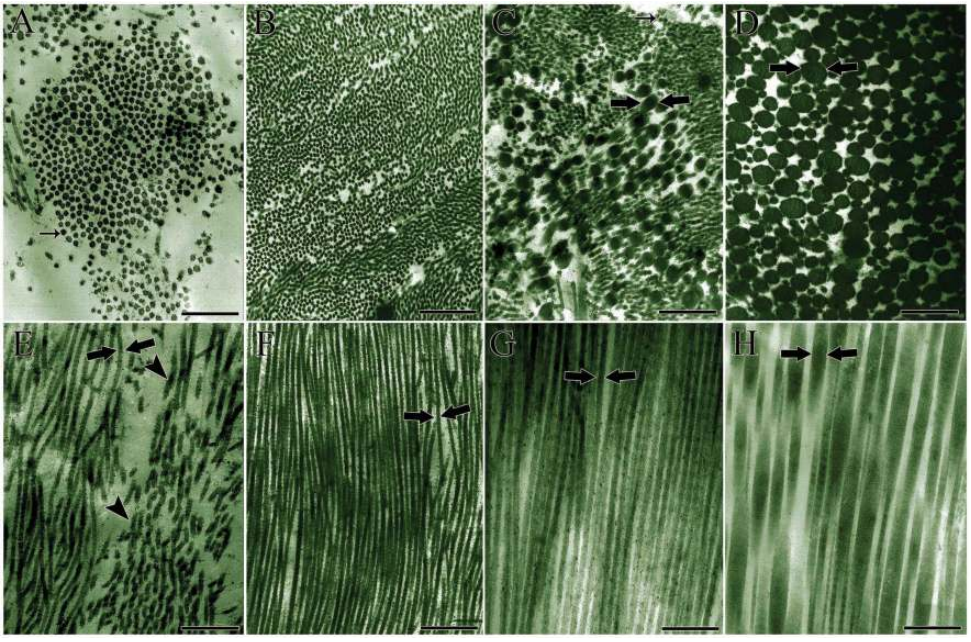

Figure 10 TEM of the injured and normal tendons at 60 DPI. (a to d) Transverse sections of the injured and normal tendons. (e to h) Longitudinal sections of the injured and normal tendons. (a and e) ICTs. (b and f) ITTCs. (c and g) ITTC-PGs. (d and h) NCTs. Treatment with CI significantly increased the number, diameter, and density of the collagen fibrils in the ITTCs when compared to the ICTs. However, the collagen fibrils were still unimodal and of small-sized diameter. In contrast to the ITTCs, the ITTC-PGs showed significantly larger diameter of the collagen fibrils so that the large collagen fibrils comparable to the normal tendon (arrows) were formed in these tendons (c). The treated tendons also had aligned collagen fibrils, so that most of the collagen fibrils (arrows) were aligned unidirectionally along the longitudinal axis of tendon. Compared to the ICTs (e), the treated tendons showed continuous collagen fibrils (f and g) while in the ICTs, the collagen fibrils were small-sized and some of them were not continuous. Scale bar: (a): 500 nm, (b) 870 nm, (c) 800 nm, (d) 600 nm, (e) 550 nm, (f) 670 nm, (g) 700 nm, (h) 650 nm. Staining: Lead citrate and uranyl acetate. (A color version of this figure is available in the online journal.)

modulus, compared to the ICTs and ITTCs ($P = 0.001$ for all). Although the ITTC-PGs had higher biomechanical properties than the controls, the measured values were still significantly lower than the normal tendons at this stage ($P = 0.001$ for all) (Figure 11).

Dry matter content. At 60 DPI, the ITTCs showed significantly higher dry matter content (more than two fold) than the ICTs ($P = 0.001$). In addition, the ITTC-PGs showed significantly higher dry matter content than the ITTCs (more than 1.5 fold) and ICTs (more than threefold) ($P = 0.001$ for both). Although the ITTC-PGs had significantly higher dry matter content than the controls, the measured values were still significantly lower than the NCTs ($33.37 \pm 2.92^{\text{ITTC-PGs}}$ % vs. $54.19 \pm 6.91^{\text{NCTs}}$ %; $P = 0.001$) at this stage (Figure 11).

Discussion

Implantation of the BPG-CI in the defect area promoted cell migration and proliferation so that the inflammatory cells diffusely infiltrated throughout the bioimplant. This resulted in the modulation of inflammation in the ITTC-PGs, which was due to the PG but not the CI. The ITTCs

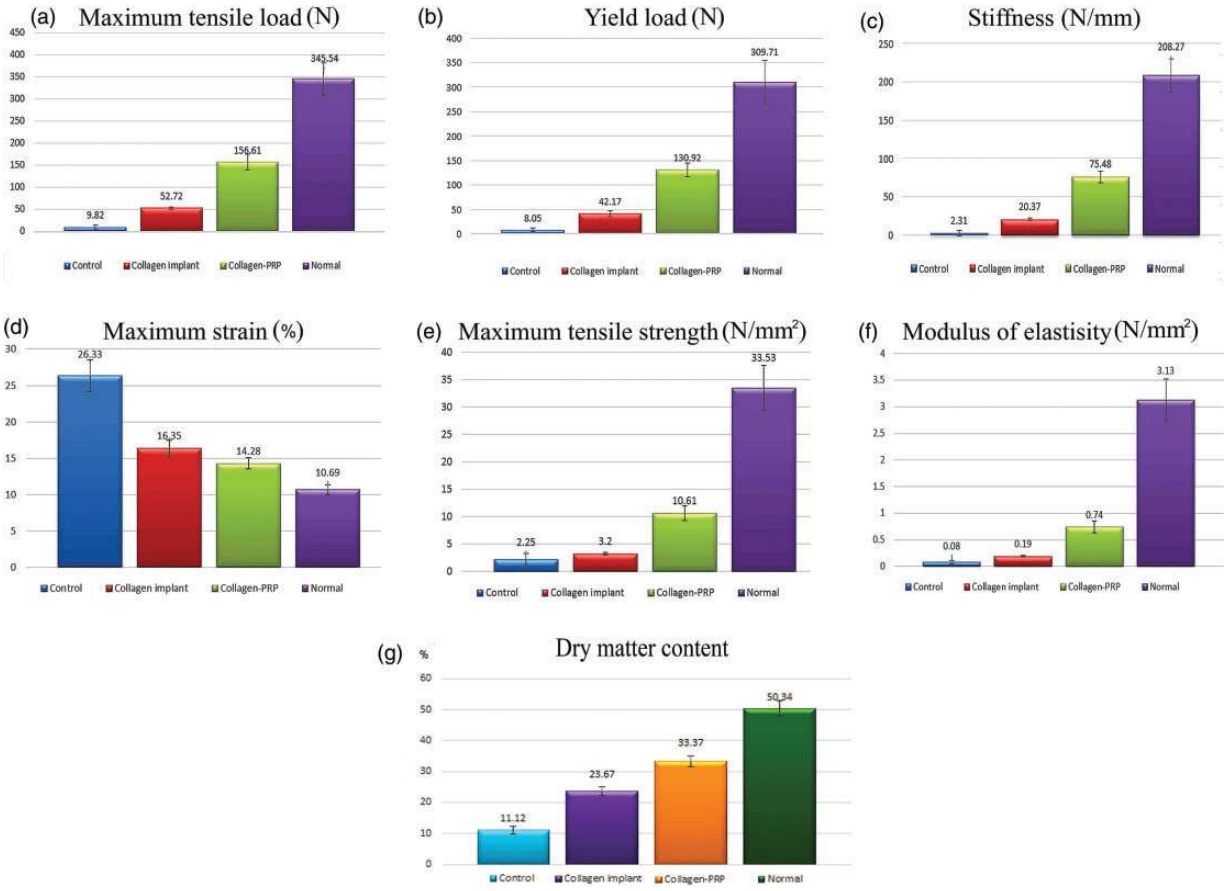

Figure 11 Biomechanical properties and dry matter content of the injured healing tendons at 60 DPI. Number of tendons in each group = 10. The results were expressed as mean ± standard deviation. (A color version of this figure is available in the online journal.)

showed a demarcation line of the infiltrated inflammatory cells around the CI: hence, most of the cells failed to access the inner parts of the implant. Thus, a continuous inflammatory reaction was observed around the CR during the fibroplasia stage. In contrast, no characteristic inflammatory response was observed in the ICTs.

Inflammation is necessary for tendon healing.[3] Without an appropriately robust inflammatory response, effective healing cannot occur.[30] During the inflammation, the inflammatory cells infiltrate the injured area, and regulate several events. Neutrophils and macrophages exert a powerful phagocytic activity and lyse the necrotic tissues and microorganisms. Macrophages also trigger cell migration, differentiation, and proliferation by their cytokines and growth factors, and facilitate the transition between inflammation and fibroplasia.[5] Lymphocytes are chronic inflammatory cells, and regulate macrophage behavior. T-helper lymphocytes type I regulate macrophages type I. Macrophages type I are mostly a phagocytic cell which could induce rejection of the implant. T-helper lymphocytes type II regulate macrophages type II. The latter exhibit less phagocytic activity but can promote remodeling reaction; thus, their activation results in graft acceptance.[3,33] Although the PG increased the inflammatory response, this inflammation terminated almost at the end of the inflammatory stage, and at fibroplasia no signs of acute inflammation were observed in the ITTC-PGs. Compared to the ITTCs, the inflammation occurring in the ITTC-PGs was mostly close to a remodeling reaction. Harris *et al*.[34] showed that PRP can initiate an inflammatory response in the absence of an inciting injury in normal soft tissues in rabbits. Also, Dragoo *et al*.[10] evaluated the inflammatory effect of two different commercially available PRP systems, Biomet GPS III leukocyte-rich PRP (LR-PRP) versus MTF Cascade leukocyte-poor PRP (LP-PRP), after intratendinous injection in rabbits. Compared with LP-PRP, LR-PRP initiated a significantly greater acute inflammatory response at 5 DPI. Our PG was free of WBCs but was xenogenous; thus, we expected such inflammation in the short term.

Bioelectricity of the tissues can determine their structural and functional features during tendon healing.[7,35] During inflammation, DTEC of a tissue increases because more electrical ions transmit through an edematous and disorganized tissue, and TRDTEC decreases because tissue organization is impaired. During fibroplasia and remodeling, DTEC decreases while TRDTEC increases; because the dry matter content and organization of the healing tissue gradually increase.[3,35] The BPG increased DTEC and reduced TRDTEC of the ITTC-PGs in the short term while it decreased the DTEC and increased the TRDTEC in the long term (60 DPI), compared to the controls.

These findings are in line with our morphologic results, suggesting that greater inflammation in the short term was associated with a better fibroplasia and remodeling at later stages.

The increase in the inflammatory response is mediated by two mechanisms. First, theoretically it is possible that the BPG were immunogenic in the rabbit, promoting florid inflammation. Second, the activated platelets have several growth factors and proinflammatory mediators which are released after implantation in the host. Hoppe *et al*.[36] showed that platelet-released growth factors enhance tenocyte proliferation and matrix synthesis *in vitro*. For this reason, we measured the PDGF and IGF-I level of the BPG *in vitro* and also the serum PDGF level of the rabbits. The PG delivered a substantially large amount of growth factors which increased cellular proliferation, migration, maturation, and matrix production *in vitro*. Also those rabbits treated with BPG-CI had significantly higher serum PDGF level than the controls. The serum PDGF level of the animals had a strong positive correlation with the dry matter content and biomechanical properties of their healing tendons and is a good indicator of the status of tendon healing. Solchaga *et al*.[37] found elevated serum levels of PDGF after implantation of Augment ® Bone Graft.

van den Dolder *et al.*[15] showed that PRP has considerable amounts of all the three isoforms of PDGF AA, -BB, -AB. Yeo *et al*.[38], in rats, treated tympanic membrane (TM) perforations with PDGF AA and showed that the AA type speeds up the healing process and prevents atrophic changes in the healed TM by promoting connective tissue growth. In a review, Hee *et al*.[39] stated that PDGF-BB is chemotactic, mitogenic, and pro-angiogenic. It regulates proliferation of tendon cells and induces extracellular matrix deposition and organization. It also improves the morphological and biomechanical properties of healing tendons and ligaments. The action of three different isoforms of PDGF on the proliferation rate and collagen synthesis of fibroblasts cultured from normal human wounds has been investigated.[40] PDGF-AA and PDGF-BB down-regulated both the steady-state levels of pro-alpha 1 (I and III) collagen chain mRNAs and the production of collagen, in a dose-dependent manner. Interestingly, PDGF-AB up-regulated the expression of type I and III procollagen mRNAs by cultured wound fibroblasts. Also, Osornio-Vargas *et al*.[41] showed that PDGF-AB and PDGF-BB are the most potent chemoattractants for Swiss 3T3 cells. Denk and Knorr[42] showed that PDGF isoforms act as mitogens for stromal fibroblasts during wound healing, when density of fibroblasts is high. The results of the ''low-density'' assays showed that PDGF AA and AB can prevent cell loss during corneal homeostasis, when the density of keratocytes is low. Gope[43] showed that topical application of PDGF-AB and PDGF-BB enhances the wound repair process in a mouse wound defect model. Finally, Pierce *et al*.[44] detected little PDGF isoform expression in normal skin and in nonhealing dermal ulcers. In contrast, in surgically produced acute wounds and chronic ulcers treated with rPDGF-BB, markedly upregulated levels of PDGF-AA were found. In both types of wounds, increased PDGF-AA was detected primarily in capillaries and fibroblasts. While PDGF-BB and PDGF-AB were present in a minority of healing wounds, they were usually present at lower levels than PDGF-AA. It seems PDGF AA may be a superior indicator of wound healing, while PDGF BB may have greater therapeutic value, and the AB type may be both therapeutic and diagnostic. We selected AA and AB types based on the available ELISA kit we used to define the PDGF level in the animals and also based on our *in vitro* findings.

Treatment with BPG-CI significantly increased angiogenicity, suggesting that optimal circulation had been established earlier than the controls. In line with our findings, in a rabbit tendon transection model, a single injection of PRP into the tendon mass significantly increases the angiogenesis at earlier stages of tendon healing.[45] Also, patients with chronic rotator cuff tears who were treated arthroscopically with leukocyte- and platelet-rich fibrin showed higher vascularization than the control group after 6 weeks.[46]

The BPG was tenoinductive, tenoconductive, and tenogenic *in vivo*. Through tenoinductivity, BPG increased tenoblast migration, proliferation, differentiation, and maturation, which increased collagen production in the neotenon. By tenoconductivity, BPG-CI guided the newly migrated cells in its architecture, promoted their proliferation along the bioimplant direction, and accelerated neotenon formation and its continuity. The bioimplant decreased the peritendinous adhesions and muscle fibrosis, suggesting that the implant was able to absorb the healing tenoblasts in its architecture and concentrate them in the defect area, guiding them to produce neotenon according to the strains imposed on it, along the muscle to bone direction. The BPG-CI was also tendinogenic, because the implant was replaced by the new tissue that had morphological and biomechanical characteristics close to a normal tendon. At 60 DPI, the new collagen fibrils in the ITTC-PGs were unidirectionally aligned along the longitudinal axis of tendon. The small-sized collagen fibrils differentiated to larger ones so that, based on their diameter, they were distributed in a multimodal pattern, resulting in four categories of collagen fibrils. The new fibrils were continuous longitudinally, with no interruption. Finally, their number and density in the ITTC-PGs were higher than the ITTCs and ICTs. These findings suggest that the new collagen fibrils were the mature form of collagen i.e. typically type I.[4,47]

The unassisted tendon healing that occurred in the ICTs failed to produce mature collagen fibrils at 60 DPI: the collagen fibrils were small (0 to 64 nm) and randomly distributed in various directions: most were interrupted, and these tendons exhibited poor biomechanical characteristics. In contrast, the collagen fibrils in the ITTCs were more organized and mature, were aligned and more continuous, and had larger transverse diameter than the ICTs so that they were distributed in a bimodal pattern (0 to 64 and 65 to 103 nm). For these reasons, the biomechanical properties of the ITTCs were significantly higher than the ICTs but lower than the ITTC-PGs because, although their fibrils were bimodal and continuous, they were not comparable to those seen in the ITTC-PGs, which had four different categories of fibrils diameter. In line with our results, in a

rabbit patellar tendon transection model, PRP gel can increase the mechanical properties of the tendon compared to controls.[48]

Treatment with BPG-CI increased tenointegration of the implant because it reduced the invasion behavior of the inflammatory cells to the CRs. Most of the remnants were well incorporated and integrated with the neotenon. Compared with the ITTCs, in the ITTC-PGs, the BPG-CI improved the acceptance rate of the remnants so that the tenoblasts and tenocytes well infiltrated in the preserved remnants at fibroplasia and remodeling phases and almost all the remnants were accepted as a part of neotenon.

The effectiveness of BPG-CI on the structure and function of the neotenon and its role in decreasing the peritendinous adhesion, muscle fibrosis, and atrophy account for the greater amount of physical activity of the treated animals compared to the controls. These beneficial effects have major clinical relevance.

Recent clinical investigations showed that autogenous platelets are not effective in tendon healing. In patients with chronic Achilles tendinopathy managed with eccentric exercises, a PRP injection compared with a saline injection did not result in greater improvement in pain and activity.[21] Also, injecting PRP for treatment of chronic midportion Achilles tendinopathy does not contribute to an increased tendon structure or alter the degree of neovascularization, compared with placebo.[20] In a cohort study, PRP application during arthroscopic rotator cuff repair does not clearly demonstrate accelerated recovery clinically or anatomically.[18] Finally Schepull *et al*.,[22] in a controlled trial, injected autologous PRP with 10 times more platelet concentration than physiologically in patients with acute Achilles tendon ruptures and showed that PRP is not a useful strategy. Despite the proven efficacy of autologous PRP on tissue regeneration in experimental studies, there is currently scanty tangible clinical evidence with respect to its efficacy in tendon disorders.[9]

Unlike clinical studies, the animal studies have used allogenous platelets for tendon healing. In a rat Achilles tendon defect model, after intrahematoma injection of allogenous concentrated platelets, the tendon callus strength and stiffness increased by about 30% after 1 week, which persisted for as long as 3 weeks after the injection.[19] Histology showed that treatment improved tendon callus maturation. Also, in a rat Achilles tendon transection model, allogenous PG significantly increases the mechanical strength of the healing tendons after 14 days. Platelets and thrombin had independent and additive stimulatory effects on tendon repair.[12] In addition, allogenous PRP is effective in the healing of tendon-from-bone supraspinatus tear model in rats because it increased fibroblastic response and vascular proliferation during the first 21 days of tendon injury but failed to improve mechanical strength of the healing tendons more than what observed for the controls.[23] Sato *et al*.[24] also investigated the role of PG on the healing of intrasynovial flexor tendons in rabbits: PG significantly increases the biomechanical properties of the healing tendons after 2 and 3 weeks of tendon injury. Finally, Matsunaga *et al*.[25] treated the partial patellar tendon defect model with allogenous compact platelet-rich fibrin, which significantly increased the ultimate failure load of the treated tendons than the controls after 12 weeks in rabbits. Although the allogenous platelets were effective in animal studies, some controversies exist.[49] In a rat Achilles tendon tear model, a single injection of PRP is not useful for tendon healing.[49]

Few studies have used xenogenous platelets for tissue healing. Human platelets have promising curative effects on healing and regeneration of rabbit radial bone defect model.[16] We showed that bovine platelets are also effective in tendon healing. Since the availability and cost-effectiveness of biomaterials are important in tissue engineering, this is one of the most important advantages of bovine platelets compared to autogenous and allogenous sources. However, the results of this study should be confirmed in future investigations. Before clinical application, it is strongly recommended to test subcutaneous biocompatibility of the BPG-CI. Perhaps, bovine thrombin, platelets, and collagen molecules should be tested for their adverse effects on human sensitivity; however, we did not observe any adverse reactions in rabbits. Perhaps, the molecular and biochemical aspects of this novel strategy could be tested in future longer term studies.

In conclusion, the BPG-CI was biocompatible, biodegradable, and effective in restoration of a neotenon in experimentally induced large Achilles tendon defect model in rabbits. BPG was able to modulate inflammation, produce a strong fibroblastic response, and contribute to remodeling of the neotenon. The bioimplant significantly increased the structural and functional characteristics of the neotenon compared to the controls ($P < 0.05$). Such bioactive graft might be an alternative option to autografts and allografts.

Author contribution: The authors had equal contribution in all parts of the study.

ACKNOWLEDGEMENT

We thank Shiraz University Veterinary School, for financial support and cooperation and much appreciate additional funding through grant ISNF 87020247, from the Iranian National Science Foundation.

REFERENCES

1. Longo UG, Lamberti A, Maffulli N, Denaro V. Tendon augmentation grafts: a systematic review. *Br Med Bull* 2010;**94**:165–88
2. Meimandi-Parizi A, Oryan A, Moshiri A. Tendon Tissue engineering and its role on healing of the experimentally induced large tendon defect model in rabbits: a comprehensive in vivo study. *PLoS ONE* 2013;**8**:e73016
3. Moshiri A, Oryan A, Meimandi-Parizi A. Role of tissue-engineered artificial tendon in healing of a large Achilles tendon defect model in rabbits. *J Am Coll Surg* 2013;**217**:421–41.e8
4. Oryan A, Moshiri A, Abdolhamid Meimandi-Parizi A, Silver IA. A long-term in vivo investigation on the effects of xenogenous based, electrospun, collagen implants on the healing of experimentally-induced large tendon defects. *J Musculoskelet Neuronal Interact* 2013;**13**:315–29
5. Sharma P, Maffulli N. Tendon injury and tendinopathy: healing and repair. *J Bone Joint Surg Am* 2005;**87**:187–202

6. Sharma P, Maffulli N. Biology of tendon injury: healing, modeling and remodeling. *J Musculoskelet Neuronal Interact* 2006;**6**:181–90
7. Meimandi-Parizi A, Oryan A, Moshiri A. Role of tissue engineered collagen based tridimensional implant on the healing response of the experimentally induced large Achilles tendon defect model in rabbits: a long term study with high clinical relevance. *J Biomed Sci* 2013;**20**:28
8. Moshiri A, Oryan A. Role of platelet rich plasma in soft and hard connective tissue healing: an evidence based review from basic to clinical application. *Hard Tissue* 2013;**2**:6
9. Kaux JF, Crielaard JM. Platelet-rich plasma application in the management of chronic tendinopathies. *Acta Orthop Belg* 2013;**79**:10–5
10. Dragoo JL, Braun HJ, Durham JL, Ridley BA, Odegaard JI, Luong R, Arnoczky SP. Comparison of the acute inflammatory response of two commercial platelet-rich plasma systems in healthy rabbit tendons. *Am J Sports Med* 2012;**40**:1274–81
11. Bielecki T, Dohan Ehrenfest DM. Platelet-rich plasma (PRP) and platelet-rich fibrin (PRF): surgical adjuvants, preparations for in situ regenerative medicine and tools for tissue engineering. *Curr Pharm Biotechnol* 2012;**13**:1121–30
12. Virchenko O, Grenegård M, Aspenberg P. Independent and additive stimulation of tendon repair by thrombin and platelets. *Acta Orthop* 2006;**77**:960–6
13. Dohan Ehrenfest DM, Bielecki T, Jimbo R, Barbé G, Del Corso M, Inchingolo F, Sammartino G. Do the fibrin architecture and leukocyte content influence the growth factor release of platelet concentrates? An evidence-based answer comparing a pure platelet-rich plasma (P-PRP) gel and a leukocyte- and platelet-rich fibrin (L-PRF). *Curr Pharm Biotechnol* 2012;**13**:1145–52
14. Weibrich G, Kleis WK, Hafner G. Growth factor levels in the platelet-rich plasma produced by 2 different methods: curasan-type PRP kit versus PCCS PRP system. *Int J Oral Maxillofac Implants* 2002;**17**:184–90
15. van den Dolder J, Mooren R, Vloon AP, Stoelinga PJ, Jansen JA. Platelet-rich plasma: quantification of growth factor levels and the effect on growth and differentiation of rat bone marrow cells. *Tissue Eng* 2006;**12**:3067–73
16. Oryan A, Meimandi Parizi A, Shafiei-Sarvestani Z, Bigham AS. Effects of combined hydroxyapatite and human platelet rich plasma on bone healing in rabbit model: radiological, macroscopical, hidtopathological and biomechanical evaluation. *Cell Tissue Bank* 2012;**13**:639–51
17. Cieslik-Bielecka A, Dohan Ehrenfest DM, Lubkowska A, Bielecki T. Microbicidal properties of Leukocyte- and Platelet-Rich Plasma/Fibrin (L-PRP/L-PRF): new perspectives. *J Biol Regul Homeost Agents* 2012;**26**:43S–52S
18. Jo CH, Kim JE, Yoon KS, Lee JH, Kang SB, Lee JH, Han HS, Rhee SH, Shin S. Does platelet-rich plasma accelerate recovery after rotator cuff repair? A prospective cohort study. *Am J Sports Med* 2011;**39**:2082–90
19. Aspenberg P, Virchenko O. Platelet concentrate injection improves Achilles tendon repair in rats. *Acta Orthop Scand* 2004;**75**:93–9
20. de Vos RJ, Weir A, Tol JL, Verhaar JA, Weinans H, van Schie HT. No effects of PRP on ultrasonographic tendon structure and neovascularisation in chronic midportion Achilles tendinopathy. *Br J Sports Med* 2011;**45**:387–92
21. de Vos RJ, Weir A, van Schie HT, Bierma-Zeinstra SM, Verhaar JA, Weinans H, Tol JL. Platelet-rich plasma injection for chronic Achilles tendinopathy: a randomized controlled trial. *JAMA* 2010;**303**:144–9
22. Schepull T, Kvist J, Norrman H, Trinks M, Berlin G, Aspenberg P. Autologous platelets have no effect on the healing of human Achilles tendon ruptures: a randomized single-blind study. *Am J Sports Med* 2011;**39**:38–47
23. Beck J, Evans D, Tonino PM, Yong S, Callaci JJ. The biomechanical and histologic effects of platelet-rich plasma on rat rotator cuff repairs. *Am J Sports Med* 2012;**40**:2037–44
24. Sato D, Takahara M, Narita A, Yamakawa J, Hashimoto J, Ishikawa H, Ogino T. Effect of platelet-rich plasma with fibrin matrix on healing of intrasynovial flexor tendons. *J Hand Surg Am* 2012;**37**:1356–63
25. Matsunaga D, Akizuki S, Takizawa T, Omae S, Kato H. Compact platelet-rich fibrin scaffold to improve healing of patellar tendon defects and for medial collateral ligament reconstruction. *Knee* 2013;**20**:545–50
26. Foltran I, Foresti E, Parma B, Sabatino P, Roveri N. Novel biologically inspired collagen nanofibres reconstituted by electrospinning method. *Macromol Symp* 2008;**269**:111–8
27. Moshiri A, Oryan A, Meimandiparizi A. A novel application of biosynthetic tissue-engineered tridimensional implant on large tendon defects: a comprehensive, detailed, in vivo investigation with significant clinical value. *Connect Tissue Res* 2013;**54**:227–43
28. Ng MH, Chai ZT, Mohd Hazlin J, Norfadila MZ, Teoh RY, ZainalAbidin SZ, Leong CF, Noor Hamidah H. Effect of freezing on the clotting and growth factor profiles of platelet-rich plasma versus platelet-poor plasma: its implication in tissue engineering. *Regen Res* 2013;**2**:48–56
29. Femia EA, Scavone M, Lecchi A, Cattaneo M. Effect of platelet count on platelet aggregation measured with impedance aggregometry (Multiplate™ analyzer) and with light transmission aggregometry. *J Thromb Haemost* 2013;**11**:2193–6
30. Oryan A, Moshiri A, Meimandi Parizi A. Implantation of a novel tissue engineered graft in a large tendon defect initiated inflammation, accelerated fibroplasia and improved remodeling of the new Achilles tendon: a comprehensive detailed study with new insights. *Cell Tissue Res* 2014;**355**:59–80
31. Oryan A, Moshiri A, Meimandiparizi A, Maffulli N. Implantation of a novel biologic and hybridized tissue engineered bioimplant in large tendon defect: an in vivo investigation. *Tissue Eng Part A* 2014;**20**:447–65
32. Czarkowska-paczek B, Bartlomiejczyk I, Przybylski J. The serum levels of growth: PDGF, TGF-BETA and VEGF are increased after strenuous physical exercise. *J Physiol Pharmacol* 2006;**57**:189–97
33. Badylak SF. Xenogeneic extracellular matrix as a scaffold for tissue reconstruction. *Transpl Immunol* 2004;**12**:367–77
34. Harris NL, Huffer WE, von Stade E, Larson AI, Phinney S, Purnell ML. The effect of platelet-rich plasma on normal soft tissues in the rabbit. *J Bone Joint Surg Am* 2012;**94**:786–93
35. Poltawski L, Watson T. Bioelectricity and microcurrent therapy for tissue healing – a narrative review. *Phys Ther Rev* 2009;**14**:104–14
36. Hoppe S, Alini M, Benneker LM, Milz S, Boileau P, Zumstein MA. Tenocytes of chronic rotator cuff tendon tears can be stimulated by platelet-released growth factors. *J Shoulder Elbow Surg* 2013;**22**:340–9
37. Solchaga LA, Daniels T, Roach S, Beasley W, Snel LB. Effect of implantation of augment (®) bone graft on serum concentrations of platelet-derived growth factors: a pharmacokinetic study. *Clin Drug Investig* 2013;**33**:143–9
38. Yeo SW, Kim SW, Suh BD, Cho SH. Effects of platelet-derived growth factor-AA on the healing process of tympanic membrane perforation. *Am J Otolaryngol* 2000;**21**:153–60
39. Hee CK, Dines JS, Solchaga LA, Shah VR, Hollinger JO. Regenerative tendon and ligament healing: opportunities with recombinant human platelet-derived growth factor BB-homodimer. *Tissue Eng Part B Rev* 2012;**18**:225–34
40. Lepistö J, Peltonen J, Vähä-Kreula M, Niinikoski J, Laato M. Platelet-derived growth factor isoforms PDGF-AA, -AB and -BB exert specific effects on collagen gene expression and mitotic activity of cultured human wound fibroblasts. *Biochem Biophys Res Commun* 1995;**209**:393–9
41. Osornio-Vargas AR, Goodell AL, Hernández-Rodríguez NA, Brody AR, Coin PG, Badgett A, Bonner JC. Platelet-derived growth factor (PDGF)-AA, -AB, and -BB induce differential chemotaxis of early-passage rat lung fibroblasts in vitro. *Am J Respir Cell Mol Biol* 1995;**12**:33–40
42. Denk PO, Knorr M. The in vitro effect of platelet-derived growth factor isoforms on the proliferation of bovine corneal stromal fibroblasts depends on cell density. *Graefes Arch Clin Exp Ophthalmol* 1997;**235**:530–4
43. Gope R. The effect of epidermal growth factor & platelet-derived growth factors on wound healing process. *Indian J Med Res* 2002;**116**:201–6
44. Pierce GF, Tarpley JE, Tseng J, Bready J, Chang D, Kenney WC, Rudolph R, Robson MC, Vande Berg J, Reid P. Detection of platelet-derived growth factor (PDGF)-AA in actively healing human wounds treated with recombinant PDGF-BB and absence of PDGF in chronic nonhealing wounds. *J Clin Invest* 1995;**96**:1336–50
45. Lyras DN, Kazakos K, Verettas D, Polychronidis A, Tryfonidis M, Botaitis S, Agrogiannis G, Simopoulos C, Kokka A, Patsouris E.

The influence of platelet-rich plasma on angiogenesis during the early phase of tendon healing. *Foot Ankle Int* 2009;**30**:1101–6
46. Zumstein MA, Rumian A, Lesbats V, Schaer M, Boileau P. Increased vascularization during early healing after biologic augmentation in repair of chronic rotator cuff tears using autologous leukocyte- and platelet-rich fibrin (L-PRF): a prospective randomized controlled pilot trial. *J Shoulder Elbow Surg* 2014;**23**:3–12
47. Oryan A, Shoushtari AH. Histology and ultrastructure of the developing Superficial Digital Flexor Tendon in rabbit. *Anat Histol Embryol* 2008;**37**:134–40
48. Lyras DN, Kazakos K, Verettas D, Botaitis S, Agrogiannis G, Kokka A, Pitiakoudis M, Kotzakaris A. The effect of platelet-rich plasma gel in the early phase of patellar tendon healing. *Arch Orthop Trauma Surg* 2009;**129**:1577–82
49. Parafioriti A, Armiraglio E, Del Bianco S, Tibalt E, Oliva F, Berardi AC. Single injection of platelet-rich plasma in a rat Achilles tendon tear model. *Muscles Ligaments Tendons J* 2011;**1**:41–7.

(Received January 24, 2014, Accepted September 8, 2014)